Truxene-Based Covalent Organic Polyhedrons Constructed through Alkyne Metathesis

SCHOLARONE™
Manuscripts

RESEARCH ARTICLE

Truxene-Based Covalent Organic Polyhedrons Constructed through Alkyne Metathesis

Xiye Yang,†[a,b] Shaofeng Huang,†[b] Michael Ortiz,[b] Xubo Wang,[b] Yunhao Cao,[a] Oula Kareem,[b] Yinghua Jin,[b] Fei Huang,[a] Xiaohui Wang,*[a] Wei Zhang*[b]

Dynamic alkyne metathesis has successfully been employed toward the synthesis of shape-persistent macrocycles and covalent organic polyhedrons (COPs). In this contribution, we present two newly designed COPs, **TC1** and **TC3**, based on truxene moiety. Specifically, the COPs were successfully synthesized under open air condition within 2 h upon heating at 55 °C with a highly active multidentate molybdenum catalyst. The fluorescent nature of truxene inspired the photoluminescence (PL) titration experiments, which demonstrate the host-guest complexation of fullerenes and the truxene based COPs with high binding constant of 10^5 M^{-1}. DFT calculations reveal the C$_{70}$@**TC1** complexation is exothermic with an enthalpy change of -102.7 kJ/mol. These findings suggest the truxene-based COPs can function as discrete fullerene acceptors, whose complexation is driven by the thermodynamics of the system. Such donor-acceptor complexation system can potentially be applied in artificial photosynthetic system development and optoelectronic application.

Covalent organic polyhedrons (COPs) with closed cage-like structures have drawn great attention owing to their fascinating unique properties and promising advances in fundamental chemistry and materials science.[1-4] COPs with shape-persistent structures are of particular interest due to their well-defined internal cavity and excellent capability of binding guest molecules with high affinity. Compared to two-dimensional (2D) macrocycle hosts with shallow well-shaped open voids, COPs have well-defined three-dimensional (3D) cavities, which can provide more confined closed space for guest molecules with higher binding interactions and selectivity (Scheme 1).[5,6] Various rigid shape-persistent COPs linked by imine bonds,[7-10] boronic esters,[11, 12] vinylenes,[13] or ethynylenes,[14-24] have been reported, and their applications in gas adsorption and separation,[8, 9, 11, 25] nanoparticle growth,[26-28] light harvesting,[29, 30] sensing,[31, 32] and catalysis[27, 33] have been demonstrated. Among them, arylene-ethynylene COPs consisting of fully unsaturated carbon backbones generally exhibit the highest shape-persistency along with high chemical and thermal stability. However, their syntheses have been challenging. Conventionally, arylene-ethynylene COPs were prepared through kinetically controlled irreversible cross coupling reactions in labor intensive multistep syntheses with low overall yields.[34] With the recent advances in dynamic alkyne metathesis, one-step efficient assembly of arylene-ethynylene COPs has been achieved through cyclooligomerization

approach under thermodynamically controlled conditions from relatively simple precursors.
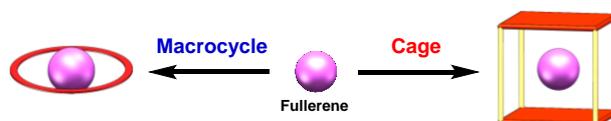
Scheme 1. Host-guest binding in a macrocycle vs. COP host.

However, there still have been relatively few accounts of arylene-ethynylene COPs with limited structural and functional diversity.[14-19] The building blocks have been limited to various substituted benzene moieties, carbazoles, and porphyrins. We envisioned incorporating conjugated moieties with strong electron donating character in an arylene-ethynylene COP would produce a novel cage structure with interesting chemical environment inside the cavity, which can accommodate various guest molecules. Truxene, a planar polycyclic aromatic hydrocarbon of C$_3$ symmetry, has been exploited for its remarkably efficient use in the design and synthesis of conjugated small molecules and polymers for optoelectronic application due to its strong electron donating ability.[35-37] This highly fluorescent molecule has seen a wide range of structural and functional group modification to improve the solubility and tune the chemical environment through side chain engineering. However, the truxene moieties have rarely been incorporated into discrete purely organic cage systems.[38-41] Herein, we report the synthesis, general spectroscopic analysis, and host-guest chemistry of bistruxene covalent organic polyhedrons prepared *via* highly efficient one-step Mo(VI) carbyne catalyzed alkyne metathesis reaction in good yields. The COPs (**TC1** and **TC3**)

a. State Key Laboratory of Pulp and Paper Engineering, State Key Laboratory of Luminescent Materials and Devices South China University of Technology Guangzhou 510640, P. R. China E-mail: fewangxh@scut.edu.cn.
b. Department of Chemistry, University of Colorado Boulder, Boulder, CO 80309, USA Email: wei.zhang@colorado.edu
†These authors contributed equally to the work.
Electronic Supplementary Information (ESI) available: DOI: 10.1039/x0xx00000x

containing two truxene panels show strong fluorescence in solution and high binding affinity toward fullerenes. Fluorescence titration experiments show that both COPs exhibit high binding constants with C_{60} and C_{70} fullerenes exceeding 10^5 M^{-1}. Furthermore, the combined fluorescence titration and DFT calculation data suggest the encapsulation of fullerene into truxene-based COPs is thermodynamically favorable, forming a 1:1 binding complex. We successfully demonstrated the construction of novel fullerene receptors by structural design, which could open new opportunities for future D-A supramolecular system development.

Previously, our group has demonstrated the use of dynamic covalent chemistry $(DC_vC)^{42}$ to synthesize a variety of two dimensional (2D) macrocycles and 3D cages through a number of reversible reactions including imine chemistry, olefin metathesis, and alkyne metathesis.[43-46] By utilizing the reversibility inherent to dynamic covalent reactions, kinetically formed species, including short oligomers and polymers, are allowed to reconstruct by breaking and reforming the covalent bonds under thermodynamically controlled conditions, effectively leading to improved yields for thermodynamically favored target macrocycles or cages. Among available dynamic covalent reactions,[42, 47, 48] we chose the reversible alkyne metathesis method for the formation of the truxene COPs due to the rigid linearity and stability of ethynylene bonds, which could provide highly stable COPs with shape-persistency and well-defined internal cavity. This is in contrast to the imine and boronic ester condensation reactions, which result in moisture sensitive bonds and more flexible cages.[12, 49] Unlike imine and boronic ester formation, which requires two complementary functional groups (e.g., amine and aldehyde for imine formation), alkyne metathesis is a self-exchange reaction without the directionality.
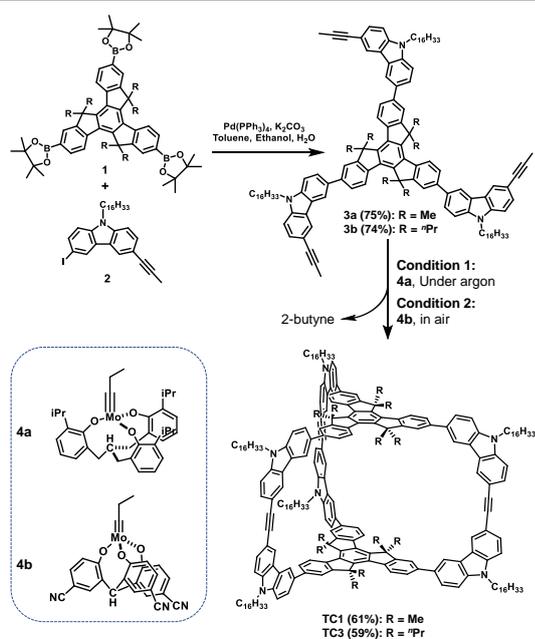
To prevent the possible complications arising from asymmetric building blocks, we designed and synthesized C_{3h} symmetric building blocks **3a**, and **3b**, which were conveniently prepared from the truxene core **1** and carbazole **2**. (Scheme 2) The carbazole units were substituted with terminal propynes that can undergo adsorption-driven alkyne metathesis. Another critical advantage of the carbazole units is the approximate 90° angle between the two substituents at 3 and 6 positions, which can provide the optimum geometry to form the target bistruxene COPs with minimal angle strain. In addition, the carbazole and truxene building blocks are equipped with alkyl groups to aid the solubility during the reaction and prevent the premature precipitation of large intermediate oligomers and polymers before their conversion to the target COPs. The synthesis of compounds **3a, 3b** were carried out under modified Suzuki-Miyaura reaction conditions through a cross-coupling between boronic ester functionalized truxene **1** and carbazole precursor **2** as shown in Scheme 2. The monomers **3a** and **3b** were then subjected to the alkyne metathesis. The highly efficient Mo(VI) carbyne catalyst **4a** consisting of a multidentate tribenzylmethine ligand was used.[50] The monomer underwent alkyne metathesis in a sealed reaction vessel under argon atmosphere at 55 °C. In the presence of molecular sieves, small alkyne byproduct, 2-butyne in this case, was simultaneously removed from the system, therefore driving the reaction equilibrium toward the product formation.[51] After 16 h, the COP **TC1** and **TC3** were formed in good isolated yields (~60 %). Recently, our group has developed a highly efficient catalysts system **4b**, which can be used in open air for a wide variety of substrates.[52] Therefore, we also tried the synthesis of **TC1** in open air using the catalyst **4b**. The mixture of the catalyst **4b** and monomer **3a** were heated in open air at 55 °C for 2 h in the absence of the molecular sieves. The byproduct 2-butyne was removed as a vapor. The GPC trace of the crude product showed that the reaction in open air under the catalysis of **4b** can provide a higher ratio of the COP **TC1** only after 2 h compared to the reaction under argon using the catalyst **4a** (Fig. 1c). Developing such user-friendly synthetic procedure for arylene-ethynylene COP formation would be of great importance for the widespread study and practical applications of cage compounds in various research fields.

The cage products **TC1** and **TC3** were characterized using ^{1}H NMR, ^{13}C NMR, and COSY spectroscopy, MALDI-TOF mass spectrometry, gel permeation chromatography (GPC), as well as steady-state UV-Vis and photoluminescence (PL) spectroscopy. The ^{1}H NMR spectrum (aromatic region shown in Fig. 1a) confirms the formation of **TC1** with a high symmetry. It should be noted that truxene faces are prochiral. When they are locked in the COP skeleton, the truxene faces become chiral with clockwise (yellow) or counter clockwise (green) chirality, which are defined by the rotation of the saturated C5, C10, and C15 carbon bridges along the C_3 axis (Fig. 1b). Therefore, there are two sets of diastereomers of **TC1**, where the two truxene faces have either the same chirality or opposite chirality. The ^{1}H NMR spectrum of **TC1** shows one set of major proton signals, along with some minor peaks likely attributed to another isomer. Two

Scheme 2 Synthesis of **TC1** and **TC3** through alkyne metathesis using the catalyst **4a** (under argon) and **4b** (in air).

sets of signals for diastereotopic methyl or methylene groups attached to C5, C10 and C15 were observed in the NMR spectra of **TC1** and **TC3** as shown in Fig. S12, S15. The MALDI-TOF mass spectrum of **TC1** supports the discrete cage formation, showing a single molecular ion peak at m/z 3256.1156 consistent with the calculated value of 3256.2788 for $C_{240}H_{288}N_6$. GPC traces in Fig. 1c, before (red) and after (black) alkyne metathesis, further confirm the isolation of a single high molecular weight species, indicating the successful formation of **TC1**. UV-Vis and photoluminescence (PL) spectroscopic techniques confirm the

presence of chromophoric truxene moieties fused within the cage structure. The fluorescence spectra of **TC1** and **TC3** are displayed in Fig. 1d. Upon excitation at the absorption band of 324 nm, PL studies revealed the characteristic emission spectrum of truxene, further supporting the incorporation of the truxenes in the COP architecture. **TC1** and **TC3** show very similar PL properties with a blue emission
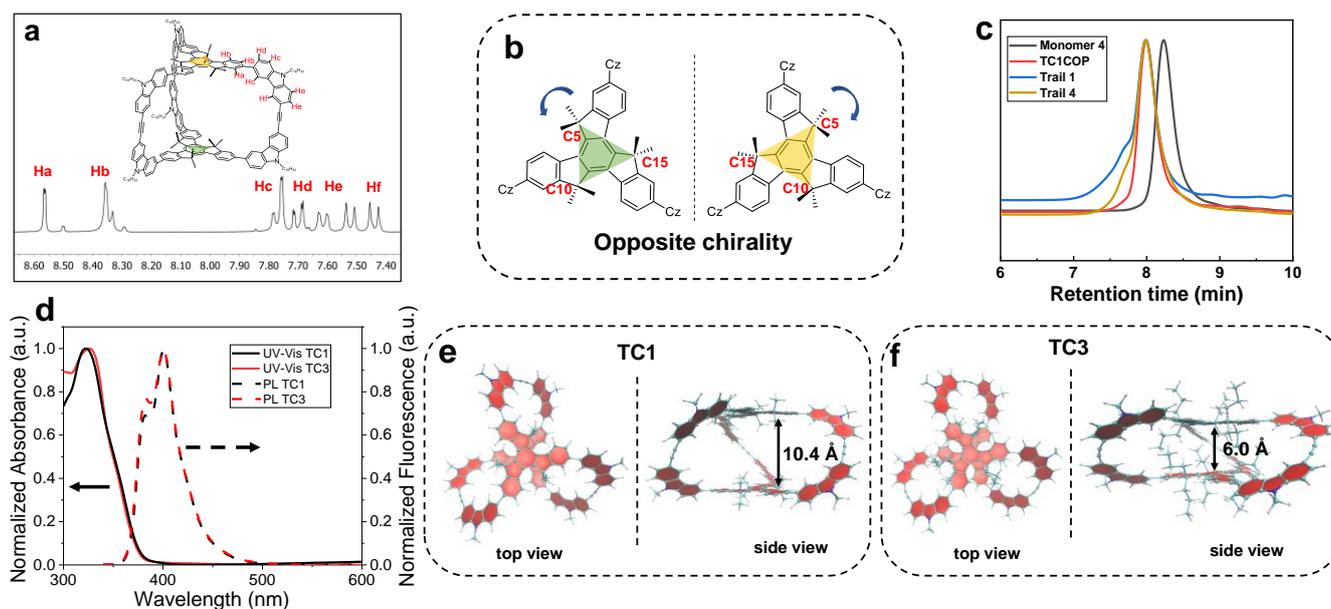

Fig. 1 TC1 characterizations: a) ^{1}H NMR of **TC1** in CDCl$_3$ with the assignment of the aromatic protons (red); b) chirality proposition of the truxene moiety for **TC1**; c) GPC trace of **TC1** and the crude products under different conditions; d) UV-Vis absorbance spectrum and PL spectrum of **TC1** (black) and **TC3** (red), both spectra recorded under exaction of 324 nm; e, f) DFT optimized structure of **TC1** (e) and **TC3** (f). Note that the alkyl chains on carbazole units are changed to methyl groups for the ease of the calculation.

at 400 nm. The negligible difference at 380 nm is probably caused by the alkyl chain length change on the truxene moiety, which could tune the molecular packing mode. Nevertheless, the strong fluorescence and narrow emission band distribution of **TC1** and **TC3**, which can be attributed to the fully conjugated cage like molecular structure.

To further identify the structure of **TC1**, we performed DFT calculation and determined the most energy favored isomer structure. Our calculation shows that the isomer composed of the truxene cores with the opposite face chirality when viewed from the top is the most energy stable product (the same exterior face chirality) (Fig. 1a). Our observation is consistent with the previously reported truxene cages,[39-41] where all the exterior faces have homochirality. However, we were unable to separate the two diastereomers using the regular column chromatography. Therefore, we tentatively assigned the major isomer as the one with homochiral exterior truxene faces. The optimized molecule structures of **TC1** and **TC3** are shown in Fig. 1e&f, respectively. Both **TC1** and **TC3** exhibit C$_3$ symmetry structures from the top view, while the substitution groups affected the molecular heights significantly from the side view.

Compared to **TC1** with methyl-substituted truxenes, the analogous molecular cage **TC3**, where the methyl groups on the truxene moiety were replaced by the longer propyl groups, shows much compressed internal cavity: the distance between top and bottom truxene panels are 10.4 Å and 6.0 Å for **TC1** and **TC3**, respectively. Likely, the longer propyl chain in **TC3** induces the CH-π interactions, leading to the more compact distorted conformation.

Of shape persistent covalent organic polyhedrons, many exhibit high guest inclusion affinities for various fullerene molecules.[14, 15] This inherent host-guest stability is driven by the rigid, aromatic, and shape-persistent cavity of COPs, which affords a thermodynamically favored complexation state with the guest. Consisting of conjugated electron donating truxene cores and the well-defined rigid cavity with a nanometer size, **TC1** and **TC3** were envisioned to be excellent hosts for fullerenes. Therefore, we performed fluorescence titration experiments with **TC1** and **TC3** to study their binding interactions with fullerenes. In a typical procedure, to a solution of the COP in toluene was added an increasing amount of the fullerene solution in toluene, and the fluorescence intensity
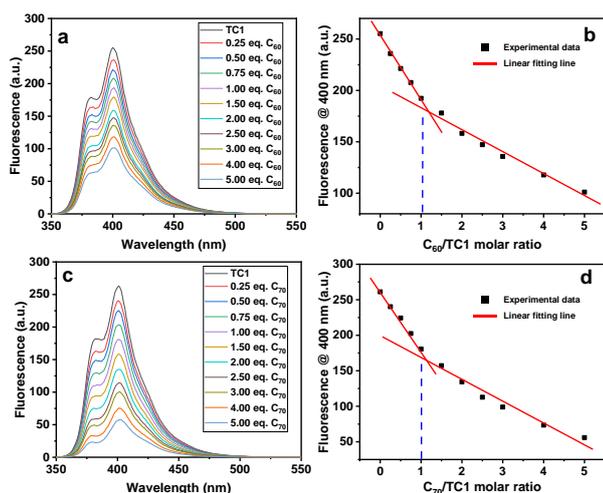
Fig. 2 Fluorescence titration of the fullerene molecules with **TC1**: (a, c) Fluorescence titration spectra of **TC1** with addition of a) C_{60} and c) C_{70}; (b, d) the plots of fluorescence intensity at 400 nm vs. equivalents of C_{60} (b) and C_{70} (d). The COP concentration (1 µM) was held constant during the titration of 25 µM solution of fullerenes. The red lines are the fitting lines.

Fig. 3 The binding constant of **TC1** with C_{60} and C_{70} compared with previously reported COP-5 and COP-6.[12,50]

change was recorded. The fluorescence titration experiments were initially conducted for **TC1** with fullerenes C_{60} and C_{70}. The fluorescence of **TC1** was strong and the quenching was very clear. As shown in Fig. 2a and 2c, gradual decrease of the fluorescence intensity was observed with the addition of the fullerene solution. The fluorescence intensity at 400 nm was then plotted against the fullerene/**TC1** molar ratio. We found the fluorescence quenching efficiency changed significantly after 1:1 host-guest ratio, suggesting a 1:1 host-guest binding mode (Fig. 3b and 3d). However, the fluorescence intensity of the mixture kept decreasing after 1 equiv. of fullerene addition. The possible reason could be the incomplete charge carrier disassociation for such donor-acceptor complex, which has usually been observed in optoelectronic heterojunction systems.[53] The binding constants of **TC1** with C_{60} and C_{70} were calculated to be 3.62 ±0.16 $*10^5$ M^{-1} and 6.70 ± 0.36 $*10^5$ M^{-1}, respectively. **TC1** has slightly stronger biding interactions with C_{70}, likely because of the better matching size of the cavity with C_{70}.

The fluorescence titration experiments were then carried out for cage **TC3** under similar conditions (Fig. S2). We found **TC3** also forms 1:1 binding complex with C_{60} and C_{70} with the binding constants of 3.18 ± 0.11 $*10^5$ M^{-1} for $C_{60}@$**TC3** and 4.76 ±0.23 $*10^5$ M^{-1} for $C_{70}@$**TC3**. Although **TC3** shows somewhat decreased binding affinities toward fullerenes when compared with **TC1**, both of them achieved high binding constants with fullerene molecules at 10^5 M^{-1} level, which is still rare in supramolecular chemistry and among the highest reported for purely organic cages.[14, 54-56] It is noteworthy that the binding constants of both **TC1** and **TC3** with C_{70} are higher than those with C_{60}, which could be attributed to the higher electron affinity of C_{70} vs. C_{60}. The cavity occupancies in the fullerene-truxene cage complexes are estimated to be 52%-58% (Table S1), which are in the optimal range (55±9 %) of volume occupancy for a stable supramolecular complex.[57] Considering
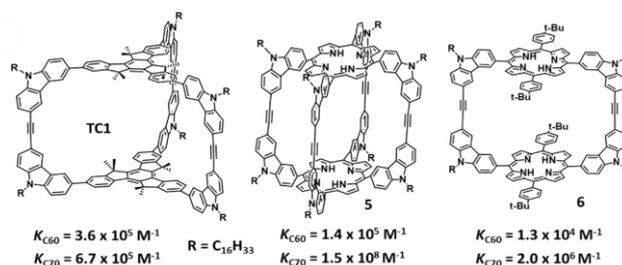
the electron donating-withdrawing effect that the complex can deliver, such truxene based molecular cage and fullerene complexes would have great application potential in various photophysical related fields.

It is interesting to note that the size of neither the guest nor the host molecules significantly influence the binding interactions of the truxene-containing cages with fullerenes. Although there is a slight preference toward the binding with C_{70}, both **TC1** and **TC3** display similarly strong interactions with C_{60} or C_{70}, showing the high binding constants in the order of 10^5 M^{-1}. This is in great contrast to our previously reported **COP-5**, which shows three orders of magnitude higher binding affinity toward C_{70} over C_{60}.[14] Another bisporphyrin **COP-6** also shows high selectivity in binding of C_{70} over C_{60} with around 150 times preference (Fig. 3).[58] **COP-5** has four pillars and a more confined internal cavity, whereas **COP-6** has only two pillars with more open macrocycle-like cavity structure. The confinement effect of **TC1**, where the cavity is surrounded by three pillars, is therefore in between the two bisporphyrin COPs. However, interestingly only a minor difference in the binding affinities toward C_{60} and C_{70} was observed. Moreover, **TC3** and **TC1**, which have considerably different initial cavity size, show similar binding interactions with C_{60} and C_{70}. These results suggest that the π-π interactions between the truxene moieties and fullerenes are likely the predominant factor controlling the fullerene binding interactions and the cavity size plays only a supporting role in these systems. Meanwhile, previously, for both **COP-5** and **COP-6**, we attributed the selective binding also to the CH-π interactions, which are well-known between fullerenes and host molecules. However, due to the larger panel sizes of **TC1** and **TC3**, the shortest distances between fullerenes and those carbazole protons pointing inside the cage are largely increased. Based on the energy-minimized structures of $C_{60}@$**TC1**, $C_{70}@$**TC1**, $C_{60}@$**TC3**, and $C_{70}@$**TC3**, the distances are measured as 4.52 Å, 5.21 Å, 3.52 Å, and 4.24 Å respectively, which all exceed the favored CH-π interaction range (2.9 Å), indicating the negligible influence of the CH-π interaction. Although C_{70} can more snugly fit inside the cage cavity and might have slightly stronger interactions with truxenes, such difference is likely not significant enough to induce a high binding selectivity toward C_{70}.

While the binding constants calculated from experimental results confirm the efficient encapsulation of fullerenes within
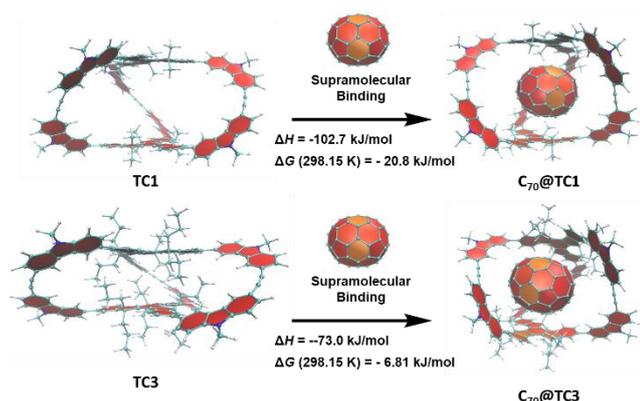
Fig. 4 Energy change of **C_{70}@TC1** and **C_{70}@TC3** formation by DFT calculation.

these cages, we also conducted theoretical calculations to better understand the energy change of the host-guest system. DFT calculation was conducted on **TC1**@C_{70} and **TC3**@C_{70} complexes. The energies of the free COP and fullerene-COP complex were calculated to compare the energy change before and after the binding (Fig. 4). We found forming C_{70}@**TC1** complex is indeed an energetically favored process, showing a negative energy change of ΔH = -102.7 kJ/mol and a negative free energy change of ΔG (298.15 K) = -20.8 kJ/mol. The calculation shows that the formation of **TC3**@C_{70} complex is also an energy favoured process with ΔH = -73.0 kJ/mol and ΔG (298.15 K) = -6.81 kJ/mol, although the distance between the top and the bottom panels is only about 6.0 Å, smaller than the size of C_{70}, in the energy minimized structure of **TC3** (Fig. 1f). Presumably, the conformational change of **TC3** from the distorted state to the fully extended one readily occurs with relatively small energy requirement. It should be noted that the kinetic effect is not considered in the calculation, since obtaining the transition state for such a process is difficult computationally.

In summary, we have successfully synthesized two novel truxene based COPs **TC1** and **TC3** through alkyne metathesis in good yields. **TC1** was also successfully obtained under open air conditions within 2 h upon heating at 55 °C using a highly active multidentate molybdenum (VI) catalyst in the absence of any 2-butyne byproduct scavenger. The COPs showed strong fluorescence and high binding constants at 10^5 M^{-1} level with fullerenes (C_{60} and C_{70}). We also used DFT calculation method to study the energy change of the COP upon binding with fullerenes. The overall energy decreased after fullerene molecule encapsulated into the COP, indicating a thermodynamically favorable process of the host-guest interaction. Our study shows that truxene-based COPs and fullerenes represent a novel host-guest system, which could find interesting applications in photophysical and optoelectronic systems.

Conflicts of interest

There are no conflicts to declare.

Notes and references

1   M. Liu, L. D. Zhang, M. A. Little, V. Kapil, M. Ceriotti, S. Y. Yang, L. F. Ding, D. L. Holden, R. Balderas-Xicohtencatl, D. L. He, R. Clowes, S. Y. Chong, G. Schutz, L. J. Chen, M. Hirscher and A. I. Cooper, Barely porous organic cages for hydrogen isotope separation, *Science*, 2019, **366**, 613-620.
2   T. Hasell and A. I. Cooper, Porous organic cages: soluble, modular and molecular pores, *Nat. Rev. Mater.*, 2016, **1**, 16053.
3   A. I. Cooper, Nanoporous Organics Enter the Cage Age, *Angew. Chem., Int. Ed.*, 2011, **50**, 996-998.
4   G. Zhang and M. Mastalerz, Organic cage compounds - from shape-persistency to function, *Chem. Soc. Rev.*, 2014, **43**, 1934-1947.
5   C. Yu, H. Long, Y. Jin and W. Zhang, Synthesis of Cyclic Porphyrin Trimers through Alkyne Metathesis Cyclooligomerization and Their Host–Guest Binding Study, *Org. Lett.*, 2016, **18**, 2946-2949.
6   C. García-Simón, M. Costas and X. Ribas, Metallosupramolecular receptors for fullerene binding and release, *Chem. Soc. Rev.*, 2016, **45**, 40-62.
7   T. Tozawa, J. T. A. Jones, S. I. Swamy, S. Jiang, D. J. Adams, S. Shakespeare, R. Clowes, D. Bradshaw, T. Hasell, S. Y. Chong, C. Tang, S. Thompson, J. Parker, A. Trewin, J. Bacsa, A. M. Z. Slawin, A. Steiner and A. I. Cooper, Porous organic cages, *Nat. Mater.*, 2009, **8**, 973-978.
8   Y. Jin, B. A. Voss, R. D. Noble and W. Zhang, A Shape-Persistent Organic Molecular Cage with High Selectivity for the Adsorption of CO2 over N2, *Angew. Chem. Int. Ed.*, 2010, **49**, 6348-6351.
9   Y. Jin, B. A. Voss, A. Jin, H. Long, R. D. Noble and W. Zhang, Highly CO2-Selective Organic Molecular Cages: What Determines the CO2 Selectivity, *J. Am. Chem. Soc.*, 2011, **133**, 6650-6658.
10 J. Koo, I. Kim, Y. Kim, D. Cho, I.-C. Hwang, R. D. Mukhopadhyay, H. Song, Y. H. Ko, A. Dhamija, H. Lee, W. Hwang, S. Kim, M.-H. Baik and K. Kim, Gigantic Porphyrinic Cages, *Chem*, 2020, **6**, 3374-3384.
11 G. Zhang, O. Presly, F. White, I. M. Oppel and M. Mastalerz, A Permanent Mesoporous Organic Cage with an Exceptionally High Surface Area, *Angew. Chem. Int. Ed.*, 2014, **53**, 1516-1520.
12 G. Zhang, O. Presly, F. White, I. M. Oppel and M. Mastalerz, A Shape-Persistent Quadruply Interlocked Giant Cage Catenane with Two Distinct Pores in the Solid State, *Angew. Chem. Int. Ed.*, 2014, **53**, 5126-5130.
13 K. D. Okochi, G. S. Han, I. M. Aldridge, Y. Liu and W. Zhang, Covalent Assembly of Heterosequenced Macrocycles and Molecular Cages through Orthogonal Dynamic Covalent Chemistry (ODCC), *Org. Lett.*, 2013, **15**, 4296-4299.

ARTICLE

Journal Name

14 C. Zhang, Q. Wang, H. Long and W. Zhang, A Highly C70 Selective Shape-Persistent Rectangular Prism Constructed through One-Step Alkyne Metathesis, *J. Am. Chem. Soc.*, 2011, **133**, 20995-21001.

15 Q. Wang, C. Zhang, B. C. Noll, H. Long, Y. Jin and W. Zhang, A Tetrameric Cage with D2h Symmetry through Alkyne Metathesis, *Angew. Chem. Int. Ed.*, 2014, **53**, 10663-10667.

16 Q. Wang, C. Yu, H. Long, Y. Du, Y. Jin and W. Zhang, Solution-Phase Dynamic Assembly of Permanently Interlocked Aryleneethynylene Cages through Alkyne Metathesis, *Angew. Chem. Int. Ed.*, 2015, **54**, 7550-7554.

17 Q. Wang, C. Yu, C. Zhang, H. Long, S. Azarnoush, Y. Jin and W. Zhang, Dynamic covalent synthesis of aryleneethynylene cages through alkyne metathesis: dimer, tetramer, or interlocked complex?, *Chem. Sci.*, 2016, **7**, 3370-3376.

18 S. Lee, A. Yang, T. P. Moneypenny and J. S. Moore, Kinetically Trapped Tetrahedral Cages via Alkyne Metathesis, *J. Am. Chem. Soc.*, 2016, **138**, 2182-2185.

19 C. C. Pattillo and J. S. Moore, A tetrahedral molecular cage with a responsive vertex, *Chem. Sci.*, 2019, **10**, 7043-7048.

20 A. Avellaneda, P. Valente, A. Burgun, J. D. Evans, A. W. Markwell-Heys, D. Rankine, D. J. Nielsen, M. R. Hill, C. J. Sumby and C. J. Doonan, Kinetically Controlled Porosity in a Robust Organic Cage Material, *Angew. Chem. Int. Ed.*, 2013, **52**, 3746-3749.

21 A. Burgun, P. Valente, J. D. Evans, D. M. Huang, C. J. Sumby and C. J. Doonan, Endohedrally functionalised porous organic cages, *Chem. Commun.*, 2016, **52**, 8850-8853.

22 S. Míguez-Lago, A. L. Llamas-Saiz, M. Magdalena Cid and J. L. Alonso-Gómez, A Covalent Organic Helical Cage with Remarkable Chiroptical Amplification, *Chem. Eur. J.*, 2015, **21**, 18085-18088.

23 S. Míguez-Lago, M. M. Cid and J. L. Alonso-Gómez, Covalent Organic Helical Cages as Sandwich Compound Containers, *Eur. J. Org. Chem.*, 2016, **2016**, 5716-5721.

24 S. Huang, Z. Lei, Y. Jin and W. Zhang, By-design molecular architectures via alkyne metathesis, *Chem. Sci.*, 2021, DOI: 10.1039/D1SC01881G.

25 M. Liu, L. Zhang, M. A. Little, V. Kapil, M. Ceriotti, S. Yang, L. Ding, D. L. Holden, R. Balderas-Xicohténcatl, D. He, R. Clowes, S. Y. Chong, G. Schütz, L. Chen, M. Hirscher and A. I. Cooper, Barely porous organic cages for hydrogen isotope separation, *Science*, 2019, **366**, 613-620.

26 R. McCaffrey, H. Long, Y. Jin, A. Sanders, W. Park and W. Zhang, Template Synthesis of Gold Nanoparticles with an Organic Molecular Cage, *J. Am. Chem. Soc.*, 2014, **136**, 1782-1785.

27 L. Qiu, R. McCaffrey, Y. Jin, Y. Gong, Y. Hu, H. Sun, W. Park and W. Zhang, Cage-templated synthesis of highly stable palladium nanoparticles and their catalytic activities in Suzuki–Miyaura coupling, *Chem. Sci.*, 2018, **9**, 676-680.

28 N. Sun, C. Wang, H. Wang, L. Yang, P. Jin, W. Zhang and J. Jiang, Multifunctional Tubular Organic Cage-Supported Ultrafine Palladium Nanoparticles for Sequential Catalysis, *Angew. Chem. Int. Ed.*, 2019, **58**, 18011-18016.

29 J. Lohrman, C. Zhang, W. Zhang and S. Ren, Semiconducting carbon nanotube and covalent organic polyhedron–C60 nanohybrids for light harvesting, *Chem. Commun.*, 2012, **48**, 8377-8379.

30 M. Ortiz, S. Cho, J. Niklas, S. Kim, O. G. Poluektov, W. Zhang, G. Rumbles and J. Park, Through-Space Ultrafast Photoinduced Electron Transfer Dynamics of a C70-Encapsulated Bisporphyrin Covalent Organic Polyhedron in a Low-Dielectric Medium, *J. Am. Chem. Soc.*, 2017, **139**, 4286-4289.

31 M. Brutschy, M. W. Schneider, M. Mastalerz and S. R. Waldvogel, Porous Organic Cage Compounds as Highly Potent Affinity Materials for Sensing by Quartz Crystal Microbalances, *Adv. Mater.*, 2012, **24**, 6049-6052.

32 K. Acharyya and P. S. Mukherjee, A fluorescent organic cage for picric acid detection, *Chem. Commun.*, 2014, **50**, 15788-15791.

33 C. Liu, K. Liu, C. Wang, H. Liu, H. Wang, H. Su, X. Li, B. Chen and J. Jiang, Elucidating heterogeneous photocatalytic superiority of microporous porphyrin organic cage, *Nat. Comm.*, 2020, **11**, 1047.

34 U. H. F. Bunz, Y. Rubin and Y. Tobe, Polyethynylated cyclic pi-systems: scaffoldings for novel two and three-dimensional carbon networks, *Chem. Soc. Rev.*, 1999, **28**, 107-119.

35 C. Huang, W. Fu, C.-Z. Li, Z. Zhang, W. Qiu, M. Shi, P. Heremans, A. K. Y. Jen and H. Chen, Dopant-Free Hole-Transporting Material with a C3h Symmetrical Truxene Core for Highly Efficient Perovskite Solar Cells, *J. Am. Chem. Soc.*, 2016, **138**, 2528-2531.

36 X.-Y. Cao, W.-B. Zhang, J.-L. Wang, X.-H. Zhou, H. Lu and J. Pei, Extended π-Conjugated Dendrimers Based on Truxene, *J. Am. Chem. Soc.*, 2003, **125**, 12430-12431.

37 K. Lin, B. Xie, Z. Wang, R. Xie, Y. Huang, C. Duan, F. Huang and Y. Cao, Star-shaped electron acceptors containing a truxene core for non-fullerene solar cells, *Org. Electron.*, 2018, **52**, 42-50.

38 J. Luo, T. Lei, X. G. Xu, F. M. Li, Y. G. Ma, K. Wu and J. Pei, Three-dimensional shape-persistent fluorescent nanocages: Facile dynamic synthesis, photophysical properties, and surface morphologies, *Chem. Eur J*, 2008, **14**, 3860-3865.

39 X. C. Wang, Y. Wang, H. Y. Yang, H. X. Fang, R. X. Chen, Y. B. Sun, N. F. Zheng, K. Tan, X. Lu, Z. Q. Tian and X. Y. Cao, Assembled molecular face-rotating polyhedra to transfer chirality from two to three dimensions, *Nat. Commun.*, 2016, **7**.

40 Y. Wang, H. X. Fang, I. Tranca, H. Qu, X. C. Wang, A. J. Markvoort, Z. Q. Tian and X. Y. Cao, Elucidation of the origin of chiral amplification in discrete molecular polyhedra, *Nat. Commun.*, 2018, **9**.

41 S. Sejourne, A. Labrunie, C. Dalinot, A. Benchohra, V. Carre, F. Aubriet, M. Allain, M. Salle and S. Goeb, Chiral Self-Sorting in Truxene-Based Metallacages, *Inorganics*, 2020, **8**.

42 Y. Jin, C. Yu, R. J. Denman and W. Zhang, Recent advances in dynamic covalent chemistry, *Chem. Soc. Rev.*, 2013, **42**, 6634-6654.

43 Y. Jin, A. Jin, R. McCaffrey, H. Long and W. Zhang, Design Strategies for Shape-Persistent Covalent Organic Polyhedrons (COPs) through Imine Condensation/Metathesis, *J. Org. Chem.*, 2012, **77**, 7392-7400.

44 K. D. Okochi, Y. Jin and W. Zhang, Highly efficient one-pot synthesis of hetero-sequenced shape-persistent macrocycles through orthogonal dynamic covalent chemistry (ODCC), *Chem. Commun.*, 2013, **49**, 4418-4420.

45 L. Zhang, Y. Jin, G.-H. Tao, Y. Gong, Y. Hu, L. He and W. Zhang, Desymmetrized Vertex Design toward a Molecular Cage with Unusual Topology, *Angew. Chem. Int. Ed.*, 2020, **59**, 20846-20851.

46 Y. Jin, Q. Wang, P. Taynton and W. Zhang, Dynamic Covalent Chemistry Approaches Toward Macrocycles, Molecular Cages, and Polymers, *Acc. Chem. Res.*, 2014, **47**, 1575-1586.

47 S. J. Rowan, S. J. Cantrill, G. R. L. Cousins, J. K. M. Sanders and J. F. Stoddart, Dynamic Covalent Chemistry, *Angew. Chem. Int. Ed.*, 2002, **41**, 898-952.

48 P. T. Corbett, J. Leclaire, L. Vial, K. R. West, J.-L. Wietor, J. K. M. Sanders and S. Otto, Dynamic Combinatorial Chemistry, *Chem. Rev.*, 2006, **106**, 3652-3711.

49 T. Hasell, X. Wu, J. T. A. Jones, J. Bacsa, A. Steiner, T. Mitra, A. Trewin, D. J. Adams and A. I. Cooper, Triply interlocked covalent organic cages, *Nat. Chem.*, 2010, **2**, 750-755.

Organic Chemistry Frontiers

50 Y. Du, H. Yang, C. Zhu, M. Ortiz, K. D. Okochi, R. Shoemaker, Y. Jin and W. Zhang, Highly Active Multidentate Ligand-Based Alkyne Metathesis Catalysts, *Chem. Eur. J.*, 2016, **22**, 7959-7963.

51 J. Heppekausen, R. Stade, R. Goddard and A. Fürstner, Practical New Silyloxy-Based Alkyne Metathesis Catalysts with Optimized Activity and Selectivity Profiles, *J. Am. Chem. Soc.*, 2010, **132**, 11045-11057.

52 Y. Ge, S. Huang, Y. Hu, L. Zhang, L. He, S. Krajewski, M. Ortiz, Y. Jin and W. Zhang, Highly active alkyne metathesis catalysts operating under open air condition, *Nat. Comm.*, 2021, **12**, 1136.

53 D. Chirvase, Z. Chiguvare, M. Knipper, J. Parisi, V. Dyakonov and J. C. Hummelen, Temperature dependent characteristics of poly(3 hexylthiophene)-fullerene based heterojunction organic solar cells, *J. Appl. Phys.*, 2003, **93**, 3376-3383.

54 M.-J. Li, C.-H. Huang, C.-C. Lai and S.-H. Chiu, Hemicarceplex Formation With a Cyclotriveratrylene-Based Molecular Cage Allows Isolation of High-Purity (≥99.0%) C70 Directly from Fullerene Extracts, *Org. Lett.*, 2012, **14**, 6146-6149.

55 Y. Shi, K. Cai, H. Xiao, Z. Liu, J. Zhou, D. Shen, Y. Qiu, Q.-H. Guo, C. Stern, M. R. Wasielewski, F. Diederich, W. A. Goddard and J. F. Stoddart, Selective Extraction of C70 by a Tetragonal Prismatic Porphyrin Cage, *J. Am. Chem. Soc.*, 2018, **140**, 13835-13842.

56 V. Leonhardt, S. Fimmel, A.-M. Krause and F. Beuerle, A covalent organic cage compound acting as a supramolecular shadow mask for the regioselective functionalization of C60, *Chem. Sci.*, 2020, **11**, 8409-8415.

57 S. Mecozzi and J. Rebek, Julius, The 55 % Solution: A Formula for Molecular Recognition in the Liquid State, *Chem. Eur. J.*, 1998, **4**, 1016-1022.

58 C. Zhang, H. Long and W. Zhang, A C84 selective porphyrin macrocycle with an adaptable cavity constructed through alkyne metathesis, *Chem. Commun.*, 2012, **48**, 6172-6174.